of the membrane vesicles produced by this bacterium showed that the membrane vesicles are enriched in active leukotoxin (Kato *et al.*, 2002; Demuth *et al.*, 2003). This would suggest that the protein association to outer membrane vesicles might be a common process among the type I secreted proteins.

The association of the α-haemolysin with the OMVs may play an important role in the pathogenicity of extraintestinal α-haemolysin-producing *E. coli* isolates, such as UPEC. The results obtained using the natural and clinical isolates confirmed that the dissemination of the α-haemolysin by OMVs is a common feature among haemolytic *E. coli* strains. *In vivo* experiments have shown the relevant role of the α-haemolysin in the pathogenicity of UPEC (Welch *et al.*, 1981; Hacker *et al.*, 1983). Moreover, *in vitro* studies indicated that the α-haemolysin has cytotoxic and/or cytolytic effects against a wide variety of cell types, including erythrocytes, neutrophils, granulocytes, epithelial cells, etc. (Lally *et al.*, 1999). Based on the present findings we suggest that OMVs may play a role in the dissemination of the α-haemolysin to the host cells and targets during extraintestinal *E. coli* infections. It will be of interest to assess their properties further and to determine the role of the OMVs carrying α-haemolysin in the pathogenicity of *E. coli* in different types of infections. The molecular events involved in delivery of the α-haemolysin from the OMVs to the eukaryotic cell is unknown at the moment. Studies on the transport of the heat-labile enterotoxin by OMVs have shown that the ETEC vesicles are internalized by an endocytic process (Kesty *et al.*, 2004). Presumably, the α-haemolysin present in OMVs could be delivered in a similar manner and further studies will hopefully clarify this question. These findings should also prompt investigations regarding the potential of other type I secreted proteins to localize to OMVs and how components of the type I secretion machinery may influence the formation and/or properties of OMVs.

Experimental procedures

Bacterial strains and plasmids

The *E. coli* strains used in this work were: MC1061 (Casadaban and Cohen, 1980), W3110 (Jensen, 1993), MG1655 (Jensen, 1993), Hb2151(Carter *et al.*, 1985), J96 (Hull *et al.*, 1982) and the isolates ER52, ER53, ER54 and ER60 (Ochman and Selander, 1984). The plasmids used were: pACYC184 (Chang and Cohen, 1978), the plasmid pANN202-312R (Godessart *et al.*, 1988) that carries the whole *hlyCABD* operon cloned in pACYC184, the plasmid pBR322 (Bolivar *et al.*, 1977), the plasmids pANN202-812 and pANN202-812B (Ludwig *et al.*, 1987) that carry the whole *hlyCABD* operon cloned in pBR322, pANN202-812B that carries a *hlyC* mutant by a frameshift in aa position 141 of HlyC, the plasmid pEHlyA (Tzschaschel *et al.*, 1996) and the plasmid pVDL9.3 (Fernandez and de Lorenzo, 2001).

Isolation of bacterial vesicles

The vesicles were isolated from bacterial cultures grown aerobically at 37°C to late log-phase in LB broth essentially as described earlier (Wai *et al.*, 1995; 2003). The isolation of OMVs was performed at late log-phase, when the expression of the α-haemolysin reaches the maximum level, as shown earlier (Mourino *et al.*, 1994). That our bacterial strains showed the same expression pattern was confirmed by determination of the amount of OMVs material and α-haemolysin through the growth curve by determination of the protein profile. Furthermore, the analysis showed that OMVs were released during all growth phases as well (data not shown). Bacterial cells were removed by centrifugation (6 000 *g*, 15 min, 4°C) and sequentially the supernatants were filtered through a 0.45 μm-pore-size vacuum filter. Vesicles were collected by ultracentrifugation (150 000 *g*, 180 min, 4°C) in a 45 Ti rotor (Beckman Instrument). The supernatants were carefully removed and the vesicles were suspended in 20 mM Tris HCl (pH 8.0), unless otherwise indicated. The absence of bacterial cells from vesicle preparations was routinely confirmed by viable count tests on L plates. Vesicles preparations were kept at –20°C.

SDS-PAGE and Western immunoblotting analyses

The standard SDS-PAGE procedure was used (Laemmli, 1970). Gels were stained with Coomassie blue or silver stain. For immunobloting, we used the methods described earlier (Towbin *et al.*, 1979). Different antibodies were used as the primary antibodies: polyclonal anti-α-haemolysin (Balsalobre *et al.*, 1996), polyclonal anti-TolC (Thanabalu *et al.*, 1998), polyclonal anti-OmpA (Henning *et al.*, 1979) and polyclonal anti-CRP (Johansson *et al.*, 2000) sera; and monoclonal anti-α-haemolysin antibody E2 (Pellett *et al.*, 1990) and monoclonal anti-E tag antibody (Amersham Biosciences). For detection we used a horseradish peroxidase-conjugate antibody and the ECL$^+$ chemiluminiscence system (Amersham Biosciences).

Dissociation assays

Vesicles in 50 mM HEPES were incubated for 60 min on ice in absence or presence of either NaCl (1 M), Na_2CO_3 (0.1 M), Urea (0.8 M) or Triton X-100 (0.5%). After incubation samples were centrifuged (20 800 *g*, 180 min, 4°C). Both soluble (supernatant) and particulate (pellet) fractions were analysed by SDS-PAGE. Prior to loading, the soluble proteins present in the supernatants were concentrated by trichloroacetic acid precipitation.

Proteinase K susceptibility assay

The proteinase K susceptibility assay was carried out as previously described (Cheng and Schneewind, 2000). Briefly, vesicles were treated at 37°C for 30 min in 20 mM Tris HCl

(pH 8.0) with proteinase K (0.5 μg ml^{-1}) in either absence or presence of 1% SDS. In parallel control experiments, 1 mM PMSF was added to inhibit the proteinase K activity. Following the incubation, all samples were placed on ice and 1 mM PMSF was added to quench all proteolysis, and the samples were analysed by SDS-PAGE.

Attachment of free α-haemolysin to OMVs

The ability of free α-haemolysin to attach to OMVs was assayed using active α-haemolysin purified by elution from SDS-polyacrylamide gel in PBS. SDS was removed by dialysis against PBS. The calcium-dependent haemolytic activity was determined as described below. A total of 5 μg of purified α-haemolysin was mixed in 50 mM HEPES with OMVs isolated from 20 ml culture supernatant from strain MC1061/pACYC184. After 30 min on ice samples were centrifuged (20 800 *g*, 180 min, 4°C). Both soluble (supernatant) and particulate (pellet) fractions were analysed by SDS-PAGE. Prior to loading, the soluble proteins present in the supernatants were concentrated by trichloroacetic acid precipitation. Control with no addition of OMVs was performed.

Cell fractionation

Cell fractions containing either the outer or the inner membranes were obtained from late log-phase cultures of MC1061/pANN202-312R in LB medium. Cells were harvested (6 000 *g*, 15 min, 4°C) and washed in HE Buffer (10 mM HEPES pH 7.8, 0.5 mM EDTA). Cells were disrupted by 1 min sonication (10 s pulses, 30% amplitude) and unbroken cells were removed by centrifugation (9 000 *g*, 5 min, 4°C). The outer and inner membrane fractions were obtained as described previously (Horstman and Kuehn, 2000).

NADH oxidase activity assay

The NADH oxidase activity of 30 μg total protein of either the vesicles or the inner and outer membrane fractions was measured as previously described (Horstman and Kuehn, 2000). The protein concentration was measured using the BCA Protein Assay Reagent Kit (Pierce).

Assay of haemolytic activity

Quantitative haemolytic assay was performed essentially as described previously (Oscarsson *et al.*, 1999). Briefly, a 20% horse blood suspension was prepared in either 0.9% NaCl or 0.9% NaCl containing 10 mM $CaCl_2$. In 96-well microtitre plates 50 μl of blood suspension was mixed with an equal amount of different dilutions of the vesicles and incubated for 60 min at 37°C. Thereafter, 100 μl of ice-cold 0.9% NaCl was added and the microtitre plate was centrifuged (400 *g*, 15 min, 4°C). The haemolytic activity was monitored as the release of haemoglobin, measured spectrophotometrically at 540 nm. The amount of vesicles in samples from strains MC1061/pACYC184 and MC1061/pANN202-312R used in the haemolytic assay was standardized by the amount of OmpA protein.

Assay for HeLa cell detachment

Cell detachment was assayed on semiconfluent monolayer of HeLa cells cultured in MEM Eagle (Sigma) with 10% fetal calf serum in 24-well tissue culture plates. HeLa cells monolayers were washed three times with PBS-CM (phosphate-buffered saline with 0.01% $CaCl_2$ and 0.01% $MgCl_2$), and 1 ml of PBS-CM was added to each well. In total, 10 μl sample (bacterial culture, culture supernatant, vesicles suspension or buffer) was added and the plate was incubated at 37°C for 90 min under 5% CO_2. Cell monolayers were washed three times with PBS-CM, fixed with 70% methanol for 10 min, stained with 0.13% crystal violet for 10 min, and then briefly destained in water. Cell detachment was quantified by eluting crystal violet with a solution of 50% ethanol and 1% SDS, and measuring the absorbance of the eluate at 590 nm. The amount of the vesicles added from MC1061/pANN202-312R was adjusted such that it contained the same amount of α-haemolysin present in 10 μl of bacterial culture. The amount of α-haemolysin present in bacterial culture and in culture supernatant after filtration was the same as estimated by SDS-PAGE (data not shown). The amount of vesicles added from control strain was adjusted by comparing the amount of OmpA in the vesicles of both MC1061/pANN202-312R and MC1061/pACYC184 strains.

Outer membrane vesicles fractionation

Assay performed as described (Horstman and Kuehn, 2000). Briefly, the OMVs were isolated as described above but suspended in 50 mM HEPES (pH 6.8), adjusted to 45% Optiprep (SIGMA) in 0.15 ml and transferred to the bottom of a 12 ml ultracentrifugation tube. Different Optiprep/HEPES layers were sequentially added as follows: 0.9 ml 35%, 0.9 ml 30%, 0.66 ml 25%, 0.66 ml 20%, 0.33 ml 15% and 0.33 ml 10%. Gradients were centrifuged (180 000 *g*, 180 min, 4°C). Fractions of equal volumes were sequentially removed and analysed by SDS-PAGE.

Electron microscopy

Ultrastructural analysis of vesicles was performed by negative staining technique as before (Wai *et al.*, 1995) using 0.5% uranyl acetate and examined by a JEM2000ET electron microscope (JEOL, Akishima, Tokyo, Japan) at 100 KV. Immunogold localization using monoclonal anti-α-haemolysin antibody E2 (Pellett *et al.*, 1990) was performed using 10 nm diameter gold particles as previously described (Wai *et al.*, 1998).

Atomic force microscopy

Outer membrane vesicles preparations were diluted with ultrapure water (Millipore) and immediately placed on a freshly cleaved mica surface. The samples were incubated at room temperature for 5 min, gently washed with ultrapure water and dried in a desiccator for at least 2 h. Imaging was performed on a Nanoscope IIIa Atomic Force Microscope (Digital Instruments) using Tapping Mode. The pictures are presented in amplitude mode.

Analysis of pulse-labelled proteins

Cultures of the strain MC1061/pANN202-312R in rich MOPS without methionine (37°C, OD_{600} of 0.7) were labelled by addition of 60 μCi [^{35}S]Methionine per millilitre (6×10^{-8} M). Incorporation of isotope was terminated at 20 s by addition of non-radioactive methionine (8×10^{-3} M). At different time points (0, 30, 60 and 300 s) after addition of non-radioactive methionine 1 ml samples were taken and soluble and vesicles fractions were separated as described above (20 800 *g*, 180 min, 4°C). The samples were analysed by SDS-PAGE.

Thin-layer chromatography

The studies on the phospholipid content were performed by TLC using Silica gel 60 plates and developing in chloroform-methanol-water (75:25:2.5, by volume). After allowing sufficient time for drying, the phospholipids were detected by spraying the plate with ethanolic phosphomolybdic acid reagent (10%), followed by charring in an oven.

Acknowledgements

We are grateful to Akemi Takade at Kyushu University for kind help with the ultrastructural analysis of the OMVs by EM, to Dr Rod Welch for monoclonal anti-HlyA antibodies and to Dr Luis A. Fernández for the plasmids pEHlyA and pVDL9.3. This work was supported by the Swedish Research Council, the Swedish Foundation for International Cooperation in Research and Higher Education (STINT), the Medical Faculty of Umeå University and The Program Ramón y Cajal of the Spanish Ministry of Education and Sciences.

References

Balsalobre, C., Juarez, A., Madrid, C., Mourino, M., Prenafeta, A., and Munoa, F.J. (1996) Complementation of the *hha* mutation in *Escherichia coli* by the *ymoA* gene from *Yersinia enterocolitica*: dependence on the gene dosage. *Microbiology* **142** (Part 7): 1841–1846.

Bauer, M.E., and Welch, R.A. (1996) Association of RTX toxins with erythrocytes. *Infect Immun* **64:** 4665–4672.

Bauer, M.E., and Welch, R.A. (1997) Pleiotropic effects of a mutation in *rfaC* on *Escherichia coli* hemolysin. *Infect Immun* **65:** 2218–2224.

Beveridge, T.J. (1999) Structures of Gram-negative cell walls and their derived membrane vesicles. *J Bacteriol* **181:** 4725–4733.

Bolivar, F., Rodriguez, R.L., Greene, P.J., Betlach, M.C., Heyneker, H.L., and Boyer, H.W. (1977) Construction and characterization of new cloning vehicles. II. A multipurpose cloning system. *Gene* **2:** 95–113.

Carter, P., Bedouelle, H., and Winter, G. (1985) Improved oligonucleotide site-directed mutagenesis using M13 vectors. *Nucleic Acids Res* **13:** 4431–4443.

Casadaban, M.J., and Cohen, S.N. (1980) Analysis of gene control signals by DNA fusion and cloning in *Escherichia coli*. *J Mol Biol* **138:** 179–207.

Chang, A.C., and Cohen, S.N. (1978) Construction and characterization of amplifiable multicopy DNA cloning vehicles derived from the P15A cryptic miniplasmid. *J Bacteriol* **134:** 1141–1156.

Cheng, L.W., and Schneewind, O. (2000) *Yersinia enterocolitica* TyeA, an intracellular regulator of the type III machinery, is required for specific targeting of YopE, YopH, YopM, and YopN into the cytosol of eukaryotic cells. *J Bacteriol* **182:** 3183–3190.

Demuth, D.R., James, D., Kowashi, Y., and Kato, S. (2003) Interaction of *Actinobacillus actinomycetemcomitans* outer membrane vesicles with HL60 cells does not require leukotoxin. *Cell Microbiol* **5:** 111–121.

Felmlee, T., and Welch, R.A. (1988) Alterations of amino acid repeats in the *Escherichia coli* hemolysin affect cytolytic activity and secretion. *Proc Natl Acad Sci USA* **85:** 5269–5273.

Fernandez, L.A., and de Lorenzo, V. (2001) Formation of disulphide bonds during secretion of proteins through the periplasmic-independent type I pathway. *Mol Microbiol* **40:** 332–346.

Fernandez, L.A., Sola, I., Enjuanes, L., and de Lorenzo, V. (2000) Specific secretion of active single-chain Fv antibodies into the supernatants of *Escherichia coli* cultures by use of the hemolysin system. *Appl Environ Microbiol* **66:** 5024–5029.

Godessart, N., Munoa, F.J., Regue, M., and Juarez, A. (1988) Chromosomal mutations that increase the production of a plasmid-encoded haemolysin in *Escherichia coli*. *J Gen Microbiol* **134:** 2779–2787.

Hacker, J., Hughes, C., Hof, H., and Goebel, W. (1983) Cloned hemolysin genes from *Escherichia coli* that cause urinary tract infection determine different levels of toxicity in mice. *Infect Immun* **42:** 57–63.

Henning, U., Schwarz, H., and Chen, R. (1979) Radioimmunological screening method for specific membrane proteins. *Anal Biochem* **97:** 153–157.

Horstman, A.L., and Kuehn, M.J. (2000) Enterotoxigenic *Escherichia coli* secretes active heat-labile enterotoxin via outer membrane vesicles. *J Biol Chem* **275:** 12489–12496.

Horstman, A.L., and Kuehn, M.J. (2002) Bacterial surface association of heat-labile enterotoxin through lipopolysaccharide after secretion via the general secretory pathway. *J Biol Chem* **277:** 32538–32545.

Hull, S.I., Hull, R.A., Minshew, B.H., and Falkow, S. (1982) Genetics of hemolysin of *Escherichia coli*. *J Bacteriol* **151:** 1006–1012.

Jensen, K.F. (1993) The *Escherichia coli* K-12 'wild types' W3110 and MG1655 have an *rph* frameshift mutation that leads to pyrimidine starvation due to low *pyrE* expression levels. *J Bacteriol* **175:** 3401–3407.

Johansson, J., Balsalobre, C., Wang, S.Y., Urbonaviciene, J., Jin, D.J., Sonden, B., and Uhlin, B.E. (2000) Nucleoid proteins stimulate stringently controlled bacterial promoters: a link between the cAMP-CRP and the (p)ppGpp regulons in *Escherichia coli*. *Cell* **102:** 475–485.

Kadurugamuwa, J.L., and Beveridge, T.J. (1995) Virulence factors are released from *Pseudomonas aeruginosa* in association with membrane vesicles during normal growth and exposure to gentamicin: a novel mechanism of enzyme secretion. *J Bacteriol* **177:** 3998–4008.

Kato, S., Kowashi, Y., and Demuth, D.R. (2002) Outer membrane-like vesicles secreted by *Actinobacillus actino-*

mycetemcomitans are enriched in leukotoxin. *Microb Pathog* **32:** 1–13.
Kesty, N.C., Mason, K.M., Reedy, M., Miller, S.E., and Kuehn, M.J. (2004) Enterotoxigenic *Escherichia coli* vesicles target toxin delivery into mammalian cells. *EMBO J* **23:** 4538–4549.
Kolling, G.L., and Matthews, K.R. (1999) Export of virulence genes and Shiga toxin by membrane vesicles of *Escherichia coli* O157:H7. *Appl Environ Microbiol* **65:** 1843–1848.
Koronakis, V. (2003) TolC – the bacterial exit duct for proteins and drugs. *FEBS Lett* **555:** 66–71.
Laemmli, U.K. (1970) Cleavage of structural proteins during the assembly of the head of bacteriophage T4. *Nature* **227:** 680–685.
Lai, X.H., Wang, S.Y., and Uhlin, B.E. (1999) Expression of cytotoxicity by potential pathogens in the standard *Escherichia coli* collection of reference (ECOR) strains. *Microbiology* **145:** 3295–3303.
Lally, E.T., Hill, R.B., Kieba, I.R., and Korostoff, J. (1999) The interaction between RTX toxins and target cells. *Trends Microbiol* **7:** 356–361.
Ludwig, A., Vogel, M., and Goebel, W. (1987) Mutations affecting activity and transport of haemolysin in *Escherichia coli*. *Mol Gen Genet* **206:** 238–245.
Moayeri, M., and Welch, R.A. (1997) Prelytic and lytic conformations of erythrocyte-associated *Escherichia coli* hemolysin. *Infect Immun* **65:** 2233–2239.
Mourino, M., Munoa, F., Balsalobre, C., Diaz, P., Madrid, C., and Juarez, A. (1994) Environmental regulation of alpha-haemolysin expression in *Escherichia coli*. *Microb Pathog* **16:** 249–259.
Nicaud, J.M., Mackman, N., Gray, L., and Holland, I.B. (1986) The C-terminal, 23 kDa peptide of *E. coli* haemolysin 2001 contains all the information necessary for its secretion by the haemolysin (Hly) export machinery. *FEBS Lett* **204:** 331–335.
Ochman, H., and Selander, R.K. (1984) Standard reference strains of *Escherichia coli* from natural populations. *J Bacteriol* **157:** 690–693.
Oropeza-Wekerle, R.L., Muller, E., Kern, P., Meyermann, R., and Goebel, W. (1989) Synthesis, inactivation, and localization of extracellular and intracellular *Escherichia coli* hemolysins. *J Bacteriol* **171:** 2783–2788.
Oscarsson, J., Mizunoe, Y., Li, L., Lai, X.H., Wieslander, A., and Uhlin, B.E. (1999) Molecular analysis of the cytolytic protein ClyA (SheA) from *Escherichia coli*. *Mol Microbiol* **32:** 1226–1238.
Pellett, S., Boehm, D.F., Snyder, I.S., Rowe, G., and Welch, R.A. (1990) Characterization of monoclonal antibodies against the *Escherichia coli* hemolysin. *Infect Immun* **58:** 822–827.
Saunders, N.B., Shoemaker, D.R., Brandt, B.L., Moran, E.E., Larsen, T., and Zollinger, W.D. (1999) Immunogenicity of intranasally administered meningococcal native outer membrane vesicles in mice. *Infect Immun* **67:** 113–119.
Shoberg, R.J., and Thomas, D.D. (1993) Specific adherence of *Borrelia burgdorferi* extracellular vesicles to human endothelial cells in culture. *Infect Immun* **61:** 3892–3900.
Stanley, P.L., Diaz, P., Bailey, M.J., Gygi, D., Juarez, A., and Hughes, C. (1993) Loss of activity in the secreted form of *Escherichia coli* haemolysin caused by an *rfaP* lesion in core lipopolysaccharide assembly. *Mol Microbiol* **10:** 781–787.
Stanley, P., Koronakis, V., and Hughes, C. (1998) Acylation of *Escherichia coli* hemolysin: a unique protein lipidation mechanism underlying toxin function. *Microbiol Mol Biol Rev* **62:** 309–333.
Thanabalu, T., Koronakis, E., Hughes, C., and Koronakis, V. (1998) Substrate-induced assembly of a contiguous channel for protein export from *E. coli*: reversible bridging of an inner-membrane translocase to an outer membrane exit pore. *EMBO J* **17:** 6487–6496.
Towbin, H., Staehelin, T., and Gordon, J. (1979) Electrophoretic transfer of proteins from polyacrylamide gels to nitrocellulose sheets: procedure and some applications. *Proc Natl Acad Sci USA* **76:** 4350–4354.
Tzschaschel, B.D., Guzman, C.A., Timmis, K.N., and de Lorenzo, V. (1996) An *Escherichia coli* hemolysin transport system-based vector for the export of polypeptides: export of Shiga-like toxin IIeB subunit by *Salmonella typhimurium aroA*. *Nat Biotechnol* **14:** 765–769.
Wai, S.N., Takade, A., and Amako, K. (1995) The release of outer membrane vesicles from the strains of enterotoxigenic *Escherichia coli*. *Microbiol Immunol* **39:** 451–456.
Wai, S.N., Mizunoe, Y., Takade, A., Kawabata, S.I., and Yoshida, S.I. (1998) *Vibrio cholerae* O1 strain TSI-4 produces exopolysaccharide materials that determine colony morphology, stress resistance, and biofilm formation. *Appl Environ Microbiol* **64:** 3648–3655.
Wai, S.N., Lindmark, B., Soderblom, T., Takade, A., Westermark, M., Oscarsson, J., *et al.* (2003) Vesicle-mediated export and assembly of pore-forming oligomers of the enterobacterial ClyA cytotoxin. *Cell* **115:** 25–35.
Wandersman, C., and Delepelaire, P. (1990) TolC, an *Escherichia coli* outer membrane protein required for hemolysin secretion. *Proc Natl Acad Sci USA* **87:** 4776–4780.
Wandersman, C., and Letoffe, S. (1993) Involvement of lipopolysaccharide in the secretion of *Escherichia coli* alpha-haemolysin and *Erwinia chrysanthemi* proteases. *Mol Microbiol* **7:** 141–150.
Welch, R.A. (1991) Pore-forming cytolysins of Gram-negative bacteria. *Mol Microbiol* **5:** 521–528.
Welch, R.A., Dellinger, E.P., Minshew, B., and Falkow, S. (1981) Haemolysin contributes to virulence of extra-intestinal *E. coli* infections. *Nature* **294:** 665–667.

Supplementary material

The following supplementary material is available for this article online:

Fig. S1. The association of HlyA with the vesicles is highly resistant to urea. Dissociation assays using vesicles from MC1061/pANN202-312R and increasing concentration of urea. Samples of vesicles in 20 mM Tris-HCl pH 8.0 with 0, 1.5 and 8 M of urea were incubated for 60 min on ice. The samples were then centrifuged and the resulting pellets (P) and supernatants (S) were analysed by 10% SDS-PAGE and silver stained. The protein band corresponding to the haemolysin is indicted with an arrowhead.

Fig. S2. The carboxi terminal domain of HlyA is not sufficient for the localization of HlyA in the OMVs. Expression of the carboxi terminal domain of HlyA from plasmid pEHlyA was

induced in different genetic backgrounds by addition of IPTG (0.25 mM; 90 min) and immunoblot analyses using anti-Etag and anti-OmpA antisera were performed. Lanes 1–4, samples from cultures of the strain Hb2151 carrying the plasmids pVDL9.3 (hlyB and hlyD) and pEHlyA (E-tagged C-HlyA); lanes 5–7, samples from cultures of the strain MC1061 carrying the plasmids pANN202-312R and pEHlyA. Lane 1: total extract before IPTG addition; lane 2 and 5: total extract after IPTG induction; lanes 3 and 6: soluble proteins precipitated from supernatant obtained after induction of EHlyA expression; lanes 4 and 7: OMVs isolated after induction of EHlyA expression.

Fig. S3. Analyses of phospholipid composition by thin-layer chromatography (TLC).
A. Total extract (lanes 1 and 2) and OMVs (lanes 3 and 4) of MC1061/pACYC184 (lanes 1 and 3) and MC1061/pANN202-312R (lanes 2 and 4); lane C: phosphatydilethanolamine.
B. Lanes 1 and 2 as in A. Lane 3: Optiprep fraction No. 9 (big OMVs, containing α-haemolysin). Lane 4: Optiprep fraction No. 15 (small OMVs).

This material is available as part of the online article from http://www.blackwell-synergy.com

Novel role of neuronal Ca^{2+} sensor-1 as a survival factor up-regulated in injured neurons

Tomoe Y. Nakamura,[1,2] Andreas Jeromin,[4] George Smith,[5] Hideaki Kurushima,[3] Hitoshi Koga,[2] Yusaku Nakabeppu,[3] Shigeo Wakabayashi,[1] and Junichi Nabekura[2,6,7]

[1]Department of Molecular Physiology, National Cardiovascular Center Research Institute, Suita, Osaka 565-8565, Japan
[2]Department of Cellular and System Physiology, Graduate School of Medical Sciences and [3]Division of Neurofunctional Genomics, Department of Immunobiology and Neuroscience, Medical Institute of Bioregulation, Kyushu University, Fukuoka 812-8582, Japan
[4]Neuroscience, Baylor College of Medicine, Houston, TX 77030
[5]Department of Physiology, University of Kentucky Medical School, Lexington, KY 50536
[6]Division of Homeostatic Development, National Institute of Physiological Sciences, Okazaki 444-8585, Japan
[7]Core Research for Evolutional Science and Technology, the Japan Science and Technology Agency, Kawaguchi, Saitama 332-0012, Japan

A molecular basis of survival from neuronal injury is essential for the development of therapeutic strategy to remedy neurodegenerative disorders. In this study, we demonstrate that an EF-hand Ca^{2+}-binding protein neuronal Ca^{2+} sensor-1 (NCS-1), one of the key proteins for various neuronal functions, also acts as an important survival factor. Overexpression of NCS-1 rendered cultured neurons more tolerant to cell death caused by several kinds of stressors, whereas the dominant-negative mutant (E120Q) accelerated it. In addition, NCS-1 proteins increased upon treatment with glial cell line–derived neurotrophic factor (GDNF) and mediated GDNF survival signal in an Akt (but not MAPK)-dependent manner. Furthermore, NCS-1 is significantly up-regulated in response to axotomy-induced injury in the dorsal motor nucleus of the vagus neurons of adult rats in vivo, and adenoviral overexpression of E120Q resulted in a significant loss of surviving neurons, suggesting that NCS-1 is involved in an antiapoptotic mechanism in adult motor neurons. We propose that NCS-1 is a novel survival-promoting factor up-regulated in injured neurons that mediates the GDNF survival signal via the phosphatidylinositol 3-kinase–Akt pathway.

Introduction

Neuronal apoptosis is induced by numerous stressors and underlies many human neurodegenerative disorders, such as Alzheimer's and Parkinson's disease. Under such apoptotic conditions, several neurotrophic factors such as glial cell line–derived neurotrophic factor (GDNF) and brain-derived neurotrophic factor (BDNF) can activate the antiapoptotic process to rescue neurons from death. However, the signaling pathway leading to cell survival is not yet completely understood. GDNF was reported to exert a potent survival-promoting activity in neurons (Henderson et al., 1994; Oppenheim et al., 1995; Yan et al., 1995) and to reduce neuronal death induced by various toxic challenges both in vitro (Nicole et al., 2001) and in vivo (Wang et al., 2002; Kirik et al., 2004). Recent evidence suggests that a part of molecular mechanisms for GDNF-induced cell survival relates to an increase in intracellular Ca^{2+} concentration, and it subsequently activates some survival pathways such as the phosphatidylinositol 3-kinase (PI3-K)–Akt pathway (Perez-Garcia et al., 2004).

Ca^{2+} is the most versatile and important intracellular messenger in neurons, regulating a variety of neuronal processes such as neurotransmission and signal transductions. The various actions of Ca^{2+} are mediated by a large family of EF-hand Ca^{2+}-binding proteins, which may act as Ca^{2+} sensors or Ca^{2+} buffers. One of them, neuronal Ca^{2+} sensor-1 (NCS-1; mammalian homologue of frequenin), was originally identified in *Drosophila melanogaster* in a screen for neuronal hyperexcitability mutants (Mallart et al., 1991). Overexpression of NCS-1 has been shown to enhance evoked neurotransmitter release and exocytosis (Pongs et al., 1993; Olafsson et al., 1995). NCS-1 directly interacts with phosphatidylinositol 4-hydroxykinase (PI4-K; Hendricks et al., 1999; Weisz et al., 2000) and enhances neuronal secretion by modulating vesicular trafficking steps in

Correspondence to Tomoe Y. Nakamura: tomoen@ri.ncvc.go.jp

Abbreviations used in this paper: BDNF, brain-derived neurotrophic factor; DMV, dorsal motor nucleus of the vagus; GAPDH, glyceraldehyde-3-phosphate dehydrogenase; GDNF, glial cell line–derived neurotrophic factor; MEK, MAPK kinase; NCS-1, neuronal Ca^{2+} sensor-1; PH, pleckstrin homology; PI3-K, phosphatidylinositol 3-kinase; PI4-K, phosphatidylinositol 4-hydroxykinase.

The Journal of Cell Biology, Vol. 172, No. 7, March 27, 2006 1081–1091
http://www.jcb.org/cgi/doi/10.1083/jcb.200508156

a phosphoinositide-dependent manner (Koizumi et al., 2002). We have previously demonstrated that NCS-1 modulates the voltage-gated K^+ channel Kv4 (Nakamura et al., 2001). Subsequently, certain voltage-gated Ca^{2+} channels have also been reported to be regulated by NCS-1 (Weiss et al., 2000; Wang et al., 2001; Tsujimoto et al., 2002). Furthermore, NCS-1 enhances the number of functional synapses (Chen et al., 2001), potentiates paired pulse facilitation (Sippy et al., 2003), and may be involved in associative learning and memory in *Caenorhabditis elegans* (Gomez et al., 2001). Despite the participation of NCS-1 in a wide range of biological functions, however, the role of NCS-1 in neuronal survival under pathophysiological conditions or the involvement of NCS-1 in neurotrophic factor–mediated neuroprotection are unknown.

Because we found that the expression levels of NCS-1 is significantly higher in immature brain (Nakamura et al., 2003) and a remarkable similarity exists between immature and injured neurons during the development and regeneration process, respectively (Nabekura et al., 2002b), these findings prompted us to study the expression level and the functional roles of NCS-1 in damaged neurons.

In this study, we found that NCS-1 is a survival-promoting factor, which increases the resistance of neurons to several kinds of stressors. In addition, NCS-1 is up-regulated in response to axonal injury in adult motor neurons, and this protects cells from apoptosis. Furthermore, NCS-1 mediates GDNF-induced neuroprotection via activation of Akt pathways. This is the first study demonstrating a novel role of NCS-1 on neuronal survival.

Results

The expression level of NCS-1 protein increases with neuronal injury

To examine the expression level of NCS-1 in injured neurons, we performed unilateral vagal axotomy (transaction of nerves) on adult rats. 1 d to 2 mo after the in vivo axotomy, brainstems, including the bilateral dorsal motor nucleus of the vagus (DMV) neurons, were isolated. Immunohistochemical staining and computerized image analysis of frozen sections revealed that axotomy significantly (more than threefold) increased the expression level of NCS-1 in the DMV when compared with those on the control side at 1 wk after the surgery (Fig. 1, A–C). NCS-1 immunoreactivity was mainly expressed in cell bodies of neurons, as shown using hematoxylin counterstaining to identify the nuclei (Fig. 1 B, brown staining accompanied with blue staining; depicted by arrows). The increase in NCS-1 level started at 1 d after axotomy, reached a peak at 1 wk, and gradually decreased to control levels over the next 2 mo (Fig. 1 D). We also conducted quantitative immunoblot analysis on tissue samples from DMV neurons 1 d and 1 wk after axotomy, expressing NCS-1 density relative to levels of glyceraldehyde-3-phosphate dehydrogenase (GAPDH). The results confirmed the immunohistochemistry experiments, with levels of NCS-1 protein in ipsilateral DMV being increased significantly (by about threefold) by 1 wk after axotomy (Fig. 1, E and F).

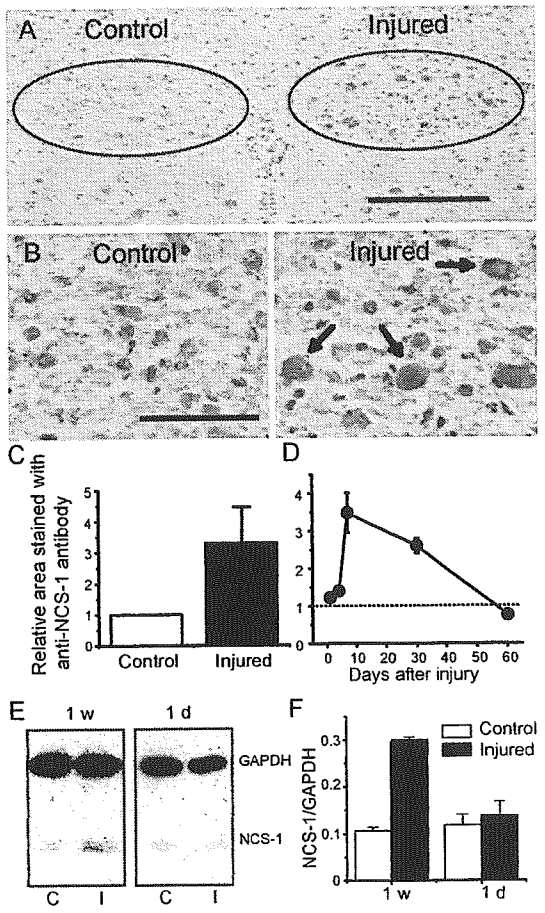

Figure 1. **NCS-1 is up-regulated in the DMV neurons after in vivo axotomy.** The 10th cranial nerve on one side of the neck of adult (4–6-wk-old) rats was cut, and, 1 d to 2 mo later, the brainstem was excised and frozen sections were cut. The NCS-1 expression was examined by counterstaining with NCS-1 antibody (brown signal) and with hematoxylin to identify nuclei (blue signal). (A) Staining pattern 1 wk after in vivo axotomy. The amount of NCS-1 protein increased in the DMV neurons ipsilateral to axotomy (injured side) when compared with control neurons contralateral to axotomy. Positions of DMV neurons are represented by circles. (B) Magnified image of DMV neurons. Arrows indicate that some neurons have both NCS-1 and hematoxylin staining, indicating that NCS-1 is expressed in cell bodies. Bars (A), 200 μm; (B) 50 μm. (C) Summarized data obtained by computerized image analysis. The relative area stained using NCS-1 antibody on the injured side 1 wk after axotomy was normalized to that of the control side (means ± SEM [error bars]; $n = 6$). (D) Time course of the expression levels of NCS-1 in injured DMV neurons relative to uninjured DMV neurons. Immunohistochemical analysis of NCS-1 levels were performed in rats 1, 4, 7, 30, and 60 d after axotomy (means ± SEM; $n = 6$). (E) Immunoblots indicating the expression levels of NCS-1 in the tissue samples obtained from DMV regions in brainstem sections at control (C) and injured sites (I) 1 wk and 1 d after axotomy. 10 sections were used for each group. Similar amount of proteins were loaded on the gel as indicated by the similar amount of the internal control GAPDH. (F) The densities of NCS-1 bands were expressed relative to the density of GAPDH bands in each tissue sample, and the group data is summarized (means ± SEM; $n = 3$).

Up-regulation of NCS-1 protein was also observed using a different type of stressor. Continuous treatment of neurons with colchicine for 4 d, which disrupts tubulin polymerization and blocks axonal transport, also increased NCS-1 expression levels (1.40 ± 0.03-fold above control levels; $P < 0.05$; $n = 4$), indicating that NCS-1 is up-regulated in vivo in response to two

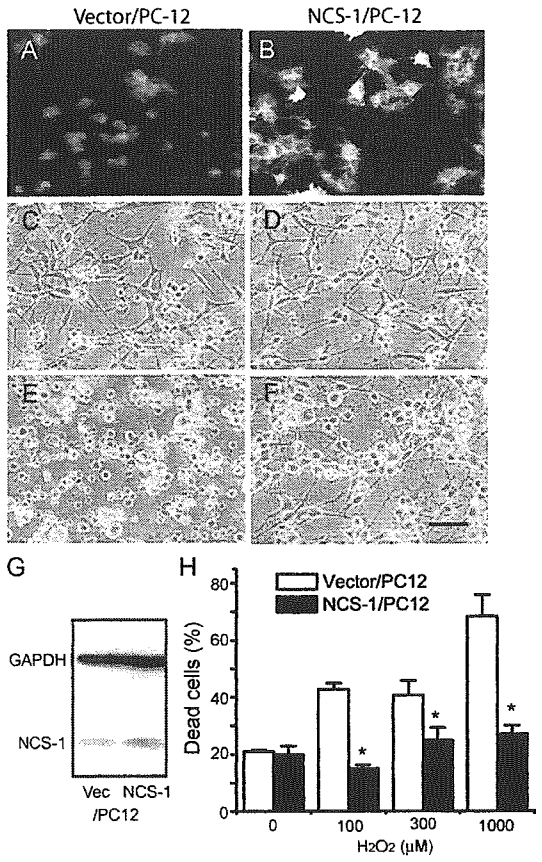

Figure 2. **Effects of the overexpression of NCS-1 on the susceptibility of PC-12 cells to H_2O_2 toxicity.** PC-12 cells stably transfected with NCS-1 (NCS-1/PC12) or vector alone (vector/PC-12) were differentiated into neuronlike cells by treatment with 100 ng/ml NGF and exposed to several concentrations (0–1 mM) of H_2O_2. (A and B) Immunofluorescent micrographs show that the expression level of NCS-1/PC12 cells is much higher than that in vector/PC12 cells. (C–F) Phase-contrast micrographs of PC-12 cells exposed to 0 (C and D) or 300 μM H_2O_2 for 3 d (E and F). Bar, 40 μm. (G) Representative immunoblots showing expression levels of NCS-1 in control vector and NCS-1–transfected cells. Also shown is the expression levels of the control protein GADPH obtained from immunoblots from the same cell samples. Unlike for NCS-1 levels, GADPH levels were not markedly different in control and NCS-1–transfected cells. (H) Bar graph shows the cell viability evaluated by trypan blue exclusion assay (means ± SEM [error bars]; $n = 8$). *, $P < 0.05$ versus vector/PC-12 cells.

different kinds of stressors—one being mechanical and the other being chemical injury.

Expression of NCS-1 renders PC-12 cells more tolerant to stressors

To study the physiological role of NCS-1 in damaged neurons, we next examined the effect of NCS-1 overexpression on the susceptibility of cells to several kinds of stressors. PC-12 cells stably transfected with either the NCS-1 expression vector (NCS-1/PC-12) or the vector alone (vector/PC-12) were differentiated into neuronlike cells, and the resistance to H_2O_2 toxicity was compared between these two groups. As shown in the immunofluorescent micrographs and immunoblot in Fig. 2 (A, B, and G), the expression level of NCS-1 was found to be significantly higher in NCS-1/PC-12 cells compared with vector-transfected cells, although these cells also had some endogenous NCS-1. Treatment with a relatively high dose (300 μM) of H_2O_2 for 3 d in the absence of pyruvate resulted in severe cellular damage in vector/PC-12 control cells; most cells were rounded up and detached from the substratum (Fig. 2 E). In contrast, the same treatment caused only a little damage to cells overexpressing NCS-1 (Fig. 2 F), indicating that the expression of NCS-1 rendered PC-12 cells more tolerant to H_2O_2 toxicity. The expression of NCS-1 reduced cell death caused by treatment with up to 1,000 μM H_2O_2 (Fig. 2 H). The aforementioned results were obtained from three cell lines transfected with NCS-1 and with corresponding vector-transfected control. A similar beneficial effect of NCS-1 on cell survival in response to 300 μM H_2O_2 was seen in two PC-12 cell lines that were not treated with NGF (not depicted).

NCS-1 promotes the long-term survival of primary cultured cortical neurons under stress and normal conditions

To further confirm the involvement of NCS-1 in neuronal survival, we overexpressed NCS-1 or its mutant E120Q in primary cultured embryonic rat cortical neurons that express endogenous NCS-1. The E120Q mutant possesses an amino acid substitution within the third EF-hand Ca^{2+}-binding motif, which impairs Ca^{2+} binding (Jeromin et al., 2004) but preserves the interaction with target proteins and, thereby, exerts a dominant-negative effect by disrupting the function of endogenous NCS-1 (Weiss et al., 2000). We used an adenoviral transfer system to transiently deliver the cDNA encoding NCS-1 together with EGFP (using an internal ribosome entry site–containing vector) and its E120Q mutant form into neurons cultured for 5 d in neurobasal medium containing B27 trophic supplements. As indicated by cells with EGFP fluorescence and nuclei stained with Hoechst 33258, nearly 70% of neurons were successfully infected with each virus at 3 d after infection (Fig. 3 A). We examined the effects of overexpression of wild-type and dominant-negative NCS-1 on neuronal survival under stress caused by B27 withdrawal, which has been reported to induce neuronal apoptosis (Brewer, 1995; Cheng et al., 2003). As shown in Fig. 3 B, B27 withdrawal promoted cell death in vector-treated control neurons (left; also compare the vector groups with and without B27 in Fig. 3 D). Overexpression of NCS-1, on the other hand, significantly rescued cells from death (Fig. 3 B, middle). In contrast, the expression of E120Q resulted in more severe cell death accompanying bleb formation (Fig. 3 B, right). To quantitatively analyze the time course for the changes in cell viability, the total number of surviving cells from the same field was counted daily by phase-contrast microscopy during 9 d (see Materials and methods). The results show that high cell viability was preserved upon expression of the wild-type NCS-1, whereas cell viability was reduced after the expression of E120Q; i.e., the number of days required to reach 70% cell viability were 5, 8, and 3 d for vector, NCS-1, and E120Q groups, respectively (Fig. 3 C). The expression levels of NCS-1 in each group of neurons before and after adenovirus infection in the absence of B27 trophic supplements are shown in the immunoblot (Fig. 3 E). Essentially the same results were obtained by counting neurons with condensed nuclei using

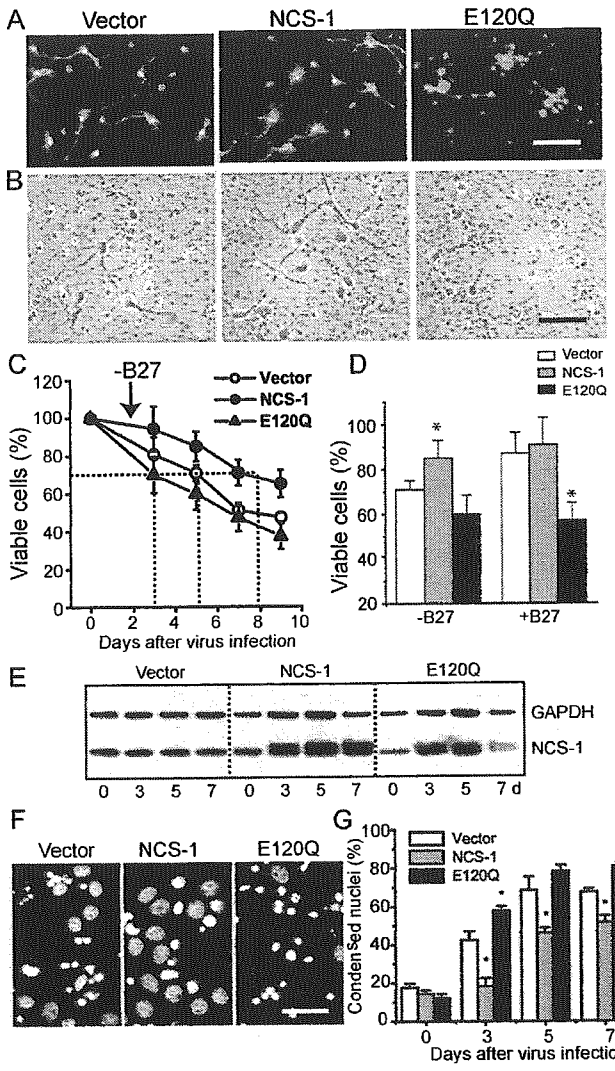

Figure 3. **Survival-promoting effect of NCS-1 in primary cultured cortical neurons.** Neurons were infected with adenovirus carrying EGFP vector alone, NCS-1, and its EF-hand mutant (E120Q) together with EGFP in the same internal ribosome entry site vector in culture medium containing neurobasal medium plus B27 trophic supplements, and they were further cultured in the presence or absence of B27 supplements (B27 supplements were withdrawn 2 d after the virus infections). (A) Fluorescent micrographs show the cultured neurons treated with adenovirus for 3 d (exhibiting strong EGFP signals) followed by treatment with a DNA-binding dye Hoechst 33258 to label their nuclei (red signals, pseudo-colored). (B) Phase-contrast micrographs show the cultured neurons treated with adenovirus for 5 d in the absence of B27 trophic supplements. Bars, 40 μm. (C) Time course of cell viability for neurons infected with adenovirus in the absence of B27 trophic supplements. Living neurons were counted daily by phase-contrast microscopy and plotted as a percentage of the initial number of neurons present on day 0 ($n = 4$). The number of days required to reach 70% cell viability is shown by the dotted lines. (D) Summary of cell viability data obtained from neurons cultured in the absence and presence of B27 trophic supplements at 5 d after virus infection. Error bars represent SEM. *, $P < 0.05$ versus the vector-controlled group. (E) Expression levels of NCS-1 and GAPDH in cultured neurons infected with each adenovirus indicated in the absence of B27 trophic supplements. (F and G) Staining patterns (light blue and white signals) of nuclei with Hoechst 33258 (F) and normalized numbers of cells having condensed nuclei (G). The dark blue color was changed to light blue or white to visualize signals more clearly. Bar, 15 μm.

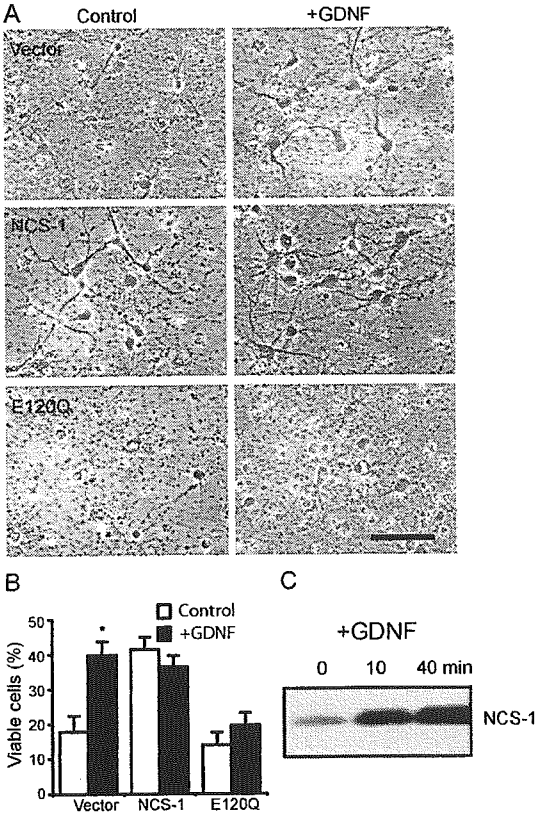

Figure 4. **NCS-1 mediates GDNF-induced neuronal survival.** (A) Primary cultured cortical neurons infected with adenovirus carrying vector alone (top), NCS-1 (middle), or E120Q mutant (bottom) were treated for 2 d with or without 10 ng/ml GDNF under the condition where B27 trophic supplement was depleted. Bar, 40 μm. (B) Summary of cell viability data. Viable cells were counted 2 d after GDNF treatment (+GDNF) or no treatment (control) and plotted as the percentage of the initial number of neurons present at day 0 in the same visual field (mean ± SEM [error bars]; $n = 4$). All neurons, not just transfected cells, were included in the cell viability counts. Note that treatment with E120Q largely prevented the GDNF-induced neuronal survival effect. *, $P < 0.05$ versus the data without exposure to GDNF. (C) Expression levels of NCS-1 in cultured neurons treated with 10 ng/ml GNDF for the indicated times.

Hoechst staining (Fig. 3, F and G), thus reinforcing the finding that the expression of NCS-1 protects neurons from cell death under apoptotic conditions. Furthermore, when B27 trophic supplement was kept in the culture medium (which is a less stress condition), the dominant-negative effect of E120Q was more clearly observed when compared with the vector control group (Fig. 3 D; also see A, where some blebs were observed in the neurons infected with E120Q mutant). In other preliminary experiments (not depicted), although the time course of the loss in cell viability was variable, overexpression of NCS-1 consistently delayed the loss of cell viability when B27 supplements were omitted, and the expression of E120Q always increased the rate of cell death when B27 was present. These results suggest that endogenous NCS-1 is playing an important role in keeping the long-term survival of cultured neurons under normal conditions in addition to the protective role from stress under apoptotic conditions.

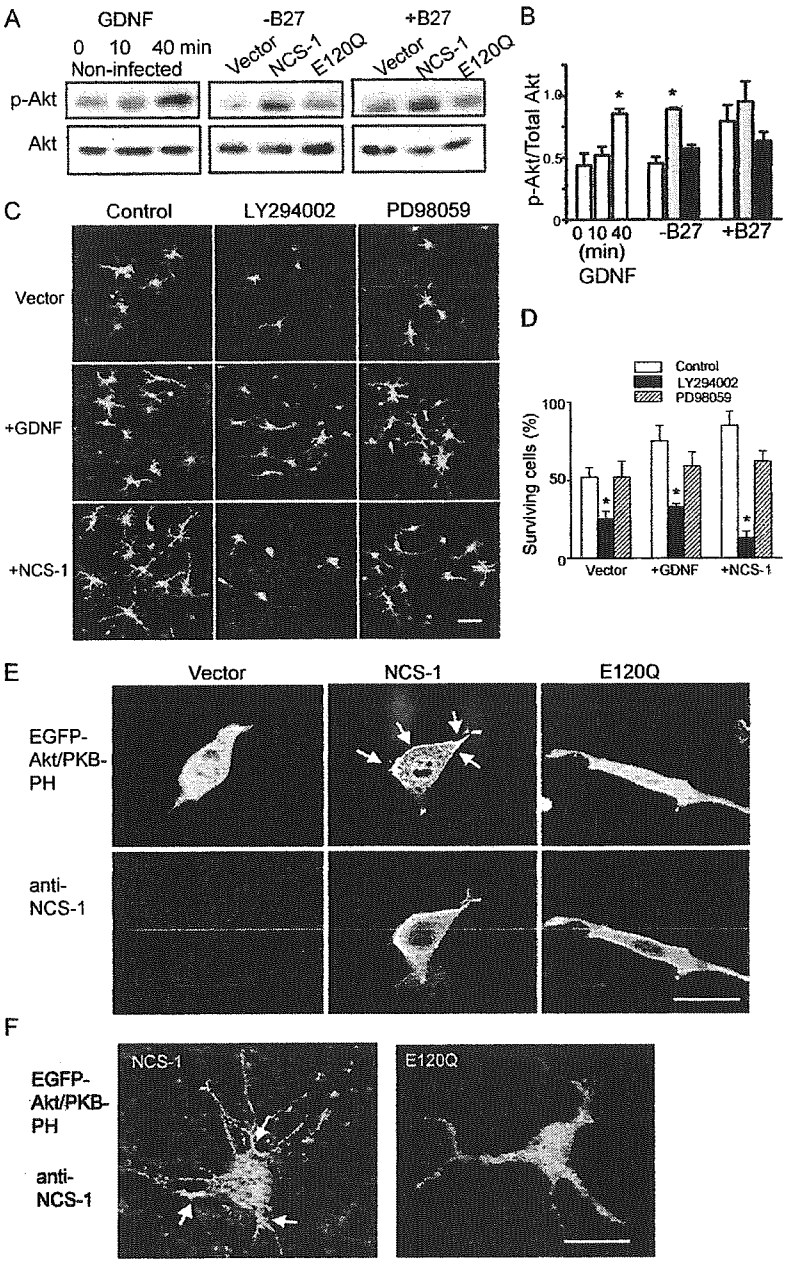

Figure 5. **NCS-1 promotes neuronal survival via activation of the PI3-K–Akt pathway.** (A and B) Both NCS-1 expression and GDNF treatment increase the phosphorylation of Akt kinase. Primary cultured cortical neurons were treated with 10 ng/ml GDNF for the indicated time periods or were infected with adenovirus carrying vector, NCS-1, or E120Q mutant and further incubated for 7 d in the presence or absence of B27 trophic supplements. They were then subjected to immunoblot analysis to detect protein levels of total (Akt) and phosphorylated form (p-Akt, the mixture of anti–P-Ser-473 and anti–P-Thr-308 antibodies, was used; A). The densities of phosphorylated Akt were normalized by those of total Akt levels and summarized in the bar graph (B). *, $P < 0.05$ versus vector control. (C and D) Both GDNF- and NCS-1–induced neuronal survival were abolished by PI3-K inhibitor but not by MEK inhibitor. Primary cultured cortical neurons were infected with adenovirus carrying NCS-1 or vector alone in medium lacking B27 trophic supplements. 3 d later, cultures were treated with 20 μM LY294002 or PD98059. For the vector-treated group, some cultures were further treated with 10 ng/ml GDNF. (C) Adenovirus-infected viable neurons treated or untreated with GDNF for 3 d. Bar, 40 μm. (D) Viable cells were counted and plotted as the percentage of the initial number of neurons present on day 0 (means ± SEM [error bars]; $n = 4$). *, $P < 0.05$ versus the data with no inhibitors. (E and F) NCS-1 activates Akt kinase by increasing the plasma membrane $PtdIns(3,4)P_2$ and $PtdIns(3,4,5)P_3$ levels in both CCL39 cells (E) and cultured neurons (F). CCL39 cells and primary cultured rat cortical neurons were transiently transfected with EGFP-Akt/PKB-PH together with either pCDNA3, NCS-1, or E120Q (1:3 ratios). 2 d later, cells were fixed, and immunocytochemistry was performed to detect NCS-1 proteins. Both EGFP distribution (E, top; and F, green signals) and NCS-1 expression (E, bottom; and F, red signals) were visualized using a laser confocal microscope. Laser confocal sections through the middle of representative cells in each treatment are shown. Arrows indicate the peripheral redistribution of the EGFP–PKB–PH in NCS-1–expressing cells. Bars, 10 μm.

NCS-1 mediates GDNF-induced cell survival

A large body of evidence suggests that neuronal survival is promoted by neurotrophic factors such as BDNF and GDNF (Boyd and Gordon, 2003). Because the long-term application of GDNF has been reported to enhance the expression of NCS-1 in *Xenopus laevis* motor neurons (Wang et al., 2001), we attempted to clarify the role of NCS-1 as a downstream mechanism of GDNF-induced cell survival in rat cortical neurons. When primary cultured cortical neurons were treated with 10 ng/ml GDNF for 2 d after the withdrawal of B27 supplements, neuronal survival was significantly enhanced when compared with time-matched control (Fig. 4, A [top] and B). Interestingly, the expression of NCS-1 mimicked the survival-promoting effects of GDNF; i.e., NCS-1 exerted a robust survival effect even in the absence of GDNF (Fig. 4, A [middle] and B). Most strikingly, the expression of the dominant-negative NCS-1 mutant E120Q largely prevented cell survival induced by GDNF (Fig. 4, A [bottom] and B). Immunoblot analysis revealed that the application of 10 ng/ml GDNF resulted in a significant increase in the expression level of endogenous NCS-1 within 10 min, which further increased at 40 min in these neurons (Fig. 4 C). The amount of NCS-1 remained elevated through 2 d of exposure to GDNF (not depicted). These results show that the treatment of GDNF increases the expression level of NCS-1, which subsequently promotes neuronal survival, suggesting that GDNF-induced neuroprotection is at least in part mediated by NCS-1.

Activation of the PI3-K-Akt pathway is involved in NCS-1-induced neuronal survival

In neurons, GDNF has been reported to promote cell survival via activation of signaling cascades involving the PI3-K–Akt pathway (Soler et al., 1999; Takahashi, 2001). In accordance with these studies, we also observed that exposure of primary cultured cortical neurons to GDNF resulted in a large increase in phospho-Akt levels (Fig. 5 A, left). Therefore, it was of interest for us to test whether NCS-1 also activates this kinase. We examined the effect of NCS-1 expression or its dominant-negative form on Akt phosphorylation in the presence or absence of B27 trophic supplements. When B27 trophic supplements were absent, the expression of NCS-1 significantly enhanced the phosphorylation of Akt, whereas expression of the dominant-negative mutant E120Q had little effect when compared with control vector-infected neurons (Fig. 5, A [middle] and B). On the other hand, when B27 supplements were present, a relatively high level of phosphorylated Akt was observed in the vector-treated control group (Fig. 5, A [right] and B). Additional expression of exogenous NCS-1 further increased the Akt phosphorylation level, whereas expression of the dominant-negative mutant suppressed phosphorylation (Fig. 5, A [right] and B). Thus, the phosphorylation levels of Akt in each group of neurons were well correlated with their viabilities, as shown in Fig. 3 D.

In addition, pretreatment of cultured cortical neurons with LY294002, an inhibitor of PI3-K, completely abolished both GDNF- and NCS-1–induced neuronal survival, whereas PD98059, an inhibitor of MAPK kinase (MEK), did not (Fig. 5, C and D). These results suggest that the NCS-1–induced survival-promoting effect is mediated via the PI3-K–Akt pathway but not the MAPK pathway in cultured cortical neurons.

To further understand the upstream mechanism of the NCS-1–induced activation of Akt, we next examined the effect of overexpression of NCS-1 and E120Q on the subcellular localization of Akt/PKB in living cells. Akt/PKB is known to be translocated to the plasma membrane when it is fully activated upon phosphorylation and bound with its substrates PtdIns(3,4)P_2 and PtdIns(3,4,5)P_3 (Alessi et al., 1996). We constructed the GFP-tagged pleckstrin homology (PH) domain of Akt/PKBα (EGFP-Akt/PKB-PH) and transiently cotransfected it into CCL39 cells, which express a small amount of endogenous NCS-1, together with NCS-1, E120Q, or empty vector. 2 d later, the subcellular localization of EGFP-tagged Akt/PKB-PH was assessed on a confocal microscope. Akt/PKB-PH was diffusely localized in the cytosol of vector-transfected control cells (Fig. 5 E). Interestingly, Akt/PKB-PH became localized in the peripheral region of cells when NCS-1 was coexpressed, but this peripheral localization was abolished when E120Q was coexpressed (Fig. 5 E). Qualitatively similar results were also obtained when primary cultured cortical neurons were treated with the same vectors; i.e., Akt/PKB-PH was localized in the peripheral regions of neurons when NCS-1 was overexpressed, but a more diffuse localization pattern was observed when E120Q was overexpressed (Fig. 5 F). The distribution pattern of Akt/PKB-PH in vector-transfected neurons was similar to that of NCS-1–overexpressing cells (not depicted). These results strongly demonstrate that NCS-1 increases the levels of plasma membrane PtdIns(3,4)P_2 and PtdIns(3,4,5)P_3 and, thus, activates Akt/PKB in living cells.

Dominant-negative NCS-1 accelerates the in vivo axotomy-induced loss of neurons

We examined the effects of the overexpression of NCS-1 and its dominant-negative mutant on the survival of these neurons to clarify the physiological role of NCS-1 in injured motor neurons in vivo. One side of vagus nerves of adult rats were axotomized as previously described (Fig. 1) and infected with adenoviral vectors encoding NCS-1, E120Q, or EGFP vector alone, and neuronal degeneration was evaluated by histological analysis. 1 wk after axotomy, nearly 30% of nerve cells were found to be EGFP positive in the injured side (Fig. 6 A). There were clear differences in the staining pattern between control and injured sides for all groups, probably because the regeneration process, such as activation of the surrounding glial cells, was ongoing on injured sides. However, the number of surviving motor neurons stained with hematoxylin were not significantly decreased at the injured side for vector-treated DMV sections (Fig. 6, B and D; examples of counted neurons are indicated by black arrows in C). This would probably be the result of natural antiapoptotic mechanisms induced by injury, which exist in mature neurons as previously reported (Benn and Woolf, 2004). Because the expression level of NCS-1 was significantly increased in response to in vivo axotomy (Fig. 1), we hypothesized that NCS-1 may be involved in this antiapoptotic mechanism. If so, blocking of endogenous NCS-1 would reduce this beneficial effect. As expected, the dominant-negative E120Q mutant resulted in a significant loss of neurons in the injured side (Fig. 6, B–D), and some TUNEL-positive nuclei were also detected only in this group (Fig. 6 E, arrows; and its magnified image in F). Considering that the infection efficiency was only ~30% in these experiments, a large majority of neurons successfully infected with E120Q appear to have undergone apoptosis. Infection of neurons with the functional NCS-1 adenovirus only had a modest effect on neuronal survival. This probably results from both the low infection efficiency and the high levels of endogenous NCS-1 expression in axotomized neurons (Fig. 1) because the NCS-1 effects are already close to maximum. Thus, the dominant-negative mutant E120Q inhibited the survival of adult DMV neurons from axotomy-induced injury, strongly suggesting that NCS-1 is one of the important factors mediating neuronal survival after in vivo axotomy.

Discussion

Numerous stressors, including physical or chemical injury and genetic abnormalities, lead to neuronal degeneration by programmed cell death along an apoptotic pathway. Under these conditions, some intrinsic and extrinsic factors, including neurotrophic factors, are known to activate the antiapoptotic process to rescue neurons from death. However, the signaling pathway leading to cell survival is not yet completely understood.

In this study, we identified a novel function for the Ca^{2+}-binding protein NCS-1, which (1) promotes the long-term survival

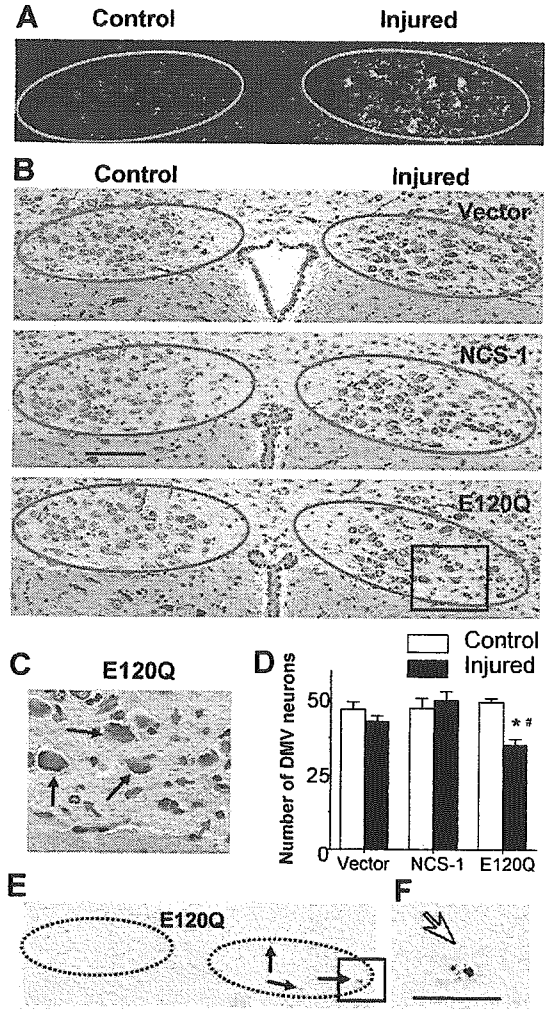

Figure 6. **Dominant-negative NCS-1 mutant E120Q promotes the axotomy-induced degeneration of DMV neurons.** After the axotomy of vagus motor neurons were performed as described in Fig.1, adenoviral vectors carrying NCS-1, E120Q, or EGFP alone were injected from the stump of the nerve. 1 wk after the treatment, the brainstem was excised, and serial sections were cut. (A) Representative EGFP fluorescence image showing that EGFP signals were detected in some cells on the injured side. Positions of DMV neurons are indicated by circles in A, B, and E. (B) Histological evaluation of DMV neurons in adenovirus-treated animals by hematoxylin/eosin staining. (C) Magnified image of the boxed area in B for E120Q-treated DMV neurons. Only neurons (indicated by black arrows), not nuclei, of glial or endothelial cells (indicated by red arrows) were counted. (D) Summarized data obtained from B. *, $P < 0.05$ versus the control side of the same section. #, $P < 0.05$ versus the injured side of vector-treated animals (means ± SEM [error bars]; $n = 6$ from three animals). (E) An example of the TUNEL-staining pattern obtained from an E120Q-treated animal. (F) The magnified image of the boxed area in E. TUNEL-positive nuclei are indicated by arrows. Bar (B), 100 μm; (F) 25 μm.

of cultured neurons via PI3-K–Akt signaling pathways; (2) mediates, at least in part, GDNF-induced neuroprotection; and (3) is up-regulated in response to axonal injury and plays an important role in the antiapoptotic mechanism in injured motor neurons.

NCS-1 is a novel survival-promoting factor in neuronal cells

We observed that the overexpression of NCS-1 rendered PC-12 cells and primary cultured cortical neurons more tolerant to several kinds of stressors, such as oxidative stress or trophic supplement withdrawal (Figs. 2 and 3), demonstrating that the expression of NCS-1 protects neurons from cell death under apoptotic conditions. In addition, overexpression of an EF-hand dominant-negative mutant E120Q significantly accelerated apoptosis when B27 trophic supplements were kept in the culture medium (Fig. 3 D), suggesting that endogenous NCS-1 is important for keeping the long-term survival of cultured neurons under normal (or less apoptotic) conditions. The latter finding also indicates that Ca^{2+} binding is required for NCS-1–mediated cell survival. On the basis of these findings, we propose that NCS-1 is a novel member of survival-promoting factors in cultured neurons.

NCS-1 mediates GDNF-induced cell survival via activation of the PI3-K-Akt survival pathway

We found that treatment of cultured cortical neurons with a neurotrophic factor GDNF increased the expression level of NCS-1 (Fig. 4 C) and enhanced neuronal survival (Fig. 4, A and B), which is consistent with a previous study reporting that GDNF enhanced the expression of frequenin/NCS-1 in *Xenopus* motor neurons (Wang et al., 2001). GDNF-induced increase in the NCS-1 level appeared to be caused by the synthesis of protein and/or mRNA but not by the prevention of NCS-1 degradation because GDNF did not raise the expression level of NCS-1 in the presence of the inhibitor of protein synthesis cycloheximide (10 μg/ml for 20 h; not depicted). In contrast to the vector-treated control neurons, GDNF did not further enhance the survival effect in neurons overexpressing NCS-1 (Fig. 4, A and B), suggesting that cell viability was already sufficiently high under this condition. Strikingly, the survival-promoting effect of GDNF was largely prevented by overexpression of the dominant-negative mutant E120Q (Fig. 4, A and B), suggesting that NCS-1 mediates the GDNF survival signal.

GDNF activates at least two intracellular pathways in neurons: one involving the PI3-K–Akt pathway and another involving the MAPK (p42 and p44, also called ERK1 and ERK2) pathway. However, PI3-K but not the MAPK pathway has been reported to be responsible for GDNF-mediated neuronal survival in motor neurons (Soler et al., 1999). In accordance with this study, we observed that exposure of primary cultured cortical neurons to GDNF resulted in a large increase in the phospho-Akt level (Fig. 5 A). In the same way, the overexpression of NCS-1 also dramatically enhanced the phosphorylation levels of Akt both in the presence and absence of B27 trophic supplements, whereas the overexpression of dominant-negative mutant E120Q did not (Fig. 5 A). In addition, the NCS-1–nduced survival-promoting effect was largely inhibited by the PI3-K inhibitor LY294002 but not the MEK inhibitor PD98059 (Fig. 5, C and D). Furthermore, NCS-1 increased the plasma membrane $PtdIns(3,4)P_2$ and $PtdIns(3,4,5)P_3$ levels, which indicates the activation of Akt in intact cells (Fig. 5, E and F). These results strongly suggest that NCS-1 is a novel downstream target that mediates GDNF survival signal through activation of the PI3-K–Akt pathway.

Possible mechanisms of the action of NCS-1

Several possible mechanisms may underlie the survival action of NCS-1. We observed that Akt/PKB-PH was recruited to the plasma membrane when NCS-1 was coexpressed, suggesting that NCS-1 acts upstream of the Akt pathway. NCS-1 was previously reported to activate PI4-K (Hendricks et al., 1999), which increases the level of plasma membrane PtdIns(4)P, the substrate of PI3-K, as well as PI5-K. Therefore, upon activation of these kinases, other phosphoinositides would be produced. Indeed, it has been reported that the overexpression of NCS-1 significantly increased both PtdIns(4)P and PtdIns(4,5)P_2 levels in PC-12 cells (Koizumi et al., 2002). Furthermore, PtdIns(3,4)P_2 and PtdIns(3,4,5)P_3, the substrates of Akt/PKB, would also be produced, which, in turn, would activate the Akt pathway (Cantley, 2002). As expected, the overexpression of NCS-1 increased the plasma membrane PtdIns(3,4)P_2 and PtdIns(3,4,5)P_3 levels both in CCL39 cells and neuronal cells (Fig. 5, E and F), enhanced the phosphorylation of Akt (Fig. 5 A), and promoted neuronal survival (Fig. 3). Therefore, we propose that activation of such a phosphatidylinositol pathway is a mechanism for the survival action of NCS-1. In addition, we observed that in contrast to GDNF, our preliminary data show that BDNF did not increase the expression level of NCS-1 (unpublished data) despite the reported survival-promoting effect of BDNF in cultured cortical neurons (Cheng et al., 2003). Interestingly, BDNF-induced survival signaling has been reported to be mediated by CaM, another Ca^{2+}-binding protein in cortical neurons (Cheng et al., 2003), and CaM has been reported to directly activate PI3-K (Perez-Garcia et al., 2004). Therefore, NCS-1 mediates the GDNF signal by activating PI4-K, whereas CaM mediates the BDNF signal by activating PI3-K. These two signals would lead the survival signal to the Akt pathway.

On the other hand, it is also possible that NCS-1 promotes neuronal survival by some other mechanisms in addition to activation of the Akt pathway. For example, the survival-promoting effect of NCS-1 appears to be analogous to that of the recently characterized antiapoptotic protein family called inhibitors of apoptosis, which suppress apoptosis through the direct inhibition of caspases (Liston et al., 2003). Some of these proteins, such as neuronal apoptosis inhibitory protein and X-linked inhibitors of apoptosis protein, have been reported to be essential for GDNF-mediated neuroprotective effects in injured motor neurons in vivo (Perrelet et al., 2002). Furthermore, recent evidence demonstrates that neuronal apoptosis inhibitory protein interacts with hippocalcin, another closely related Ca^{2+}-binding protein that affects caspase-12 activity (Korhonen et al., 2005) and protects neurons against Ca^{2+}-induced cell death (Mercer et al., 2000). Therefore, we do not exclude the possibility that like these proteins, NCS-1 also exerts a more direct effect on some caspases. We are currently investigating the possible interaction of these proteins.

As NCS-1 is known to interact with voltage-gated K^+ channels (Kv4; Nakamura et al., 2001), it might also increase the resistance of neurons to excitotoxic apoptosis through the activation of K^+ channels. Increased outward K^+ current would prevent neurons from reaching firing threshold and, thereby, prevent cells from Ca^{2+} overload leading to cell death.

NCS-1 is a novel survival-promoting factor up-regulated in injured neurons

In this study, we found that the expression level of NCS-1 was significantly increased in response to axonal injuries (transection of the vagus nerve as well as treatment of nerves with colchicine) in the DMV neurons of adult rats (Fig. 1). The behavior of NCS-1 appears to be analogous to that of the recently identified protein damage-induced neuronal endopeptidase, which is expressed in response to neuronal damages induced by nerve transection and colchicine treatment in both the central and peripheral nervous systems (Kiryu-Seo et al., 2000). Because antiapoptotic mechanisms are activated in mature neurons in response to stress to protect against accidental apoptotic cell death, it has been described that peripheral axotomy in adult neurons does not result in extensive cell death (Benn and Woolf, 2004). In accordance with this, we also observed that little loss of motor neurons was evident by in vivo axotomy in vector-treated control neurons (Fig. 6, B and D). The expression of exogenous NCS-1 did not exert the further beneficial effect (Fig. 6, B and D). This marginal effect of exogenous NCS-1 (compared with the vector control group) would be the result of the increased expression level of endogenous NCS-1 in axotomized neurons, which occurs for all groups. In contrast, overexpression of dominant-negative E120Q significantly decreased the number of surviving neurons (Fig. 6, B–D) and produced TUNEL-positive apoptotic neurons at the injured side (Fig. 6, E and F), indicating that disruption of NCS-1 function increased the vulnerability of DMV neurons to axotomy.

Overexpression of NCS-1 rendered PC-12 cells resistant to H_2O_2 toxicity even in the absence of GDNF (Fig. 2), suggesting that NCS-1 itself is enough to promote cell survival. This is consistent with our view that NCS-1 is the downstream target for GDNF. Because growing evidence indicates that nerve injury leads to the up-regulation of multiple antiapoptotic molecules, including GDNF (Liberatore et al., 1997; Yamamoto et al., 1998; Wang et al., 2002), it is possible that neuronal damages induced by in vivo axotomy enhance the synthesis and/or secretion of GDNF, which, in turn, up-regulates NCS-1 expression and promotes neuronal survival in injured neurons. Although an underlying mechanism would be different, the up-regulation of NCS-1 has also been reported in the cortex of schizophrenic and bipolar patients, demonstrating the involvement of NCS-1 in neurological disease (Koh et al., 2003).

In conclusion, we characterized a novel function of NCS-1 mediating a GDNF-induced neuroprotective effect via activations of Akt kinase. Furthermore, we found that NCS-1 is up-regulated in response to nerve injury and plays an important role in the antiapoptotic mechanism in adult motor neurons. Our present findings would provide new and basic insights into the mechanism of neuronal regeneration.

Materials and methods

Plasmids and viral vectors

E120Q NCS-1 point mutant was generated with a conventional PCR protocol using the wild-type rat NCS-1 (GenBank/EMBL/DDBJ accession no. L27421 as a template and was sequenced to confirm the mutation.

Akt/PKBα cDNA was cloned from the human kidney cDNA library (CLONTECH Laboratories, Inc.), and NH_2-terminally tagged fluorescent protein EGFP-Akt/PKB-PH was constructed incorporating a fragment of 750 bp, encoding the first 250 amino acids of PKBα (containing the PH domain) into EGFP-vector as described previously (Currie et al., 1999).

Adenovirus containing wild-type NCS-1 and the E120Q mutant inserts were generated by cotransfecting either of these plasmids and pBHG11 (Microbix Biosystems, Inc.) into HEK 293 cells. Viral DNA was isolated from the supernatant in the wells displaying the cytopathic effect. Replication-incompetent virus containing DNA inserts were plaque-purified twice and grown on HEK 293 cells to produce large amounts of adenovirus. Tissue culture supernatant containing adenovirus was concentrated by centrifugation over cesium chloride. The titers of viral stocks were 2.2×10^{10} pfu/ml for EGFP–NCS-1, 1.1×10^{10} pfu/ml for EGFP-E120Q, and 2.2×10^{10} pfu/ml for EGFP-vector.

Cell cultures

PC-12 cells stably transfected with vector alone or vector containing cDNA coding for the wild-type NCS-1 (several clones) were grown onto collagen-coated (500 μg/ml of type I; Sigma-Aldrich) culture dishes in growth medium (DME containing 10% horse serum, 5% FBS, and 400 μg/ml geneticin and gentamicin) as described previously (Koizumi et al., 2002). When cells became 80% confluent, they were switched to the differentiation medium (growth medium with half serum) supplemented with 100 ng/ml NGF-7S (Invitrogen).

Primary culture of cortical neurons was performed using the cortex from Sprague-Dawley rats at embryonic day 18. In brief, cortical tissues were isolated from whole brain, minced into small pieces, and digested for 10 min at 37°C in a 20-U/ml papain solution containing 0.002% DNase I (Worthington Biochemical Corp.). After titration of the enzymatic activity, cells were mechanically dissociated by several passages through pipette tips. After centrifugation, cells were resuspended in neurobasal medium supplemented with B27 trophic factors (both from Invitrogen), whose compositions were reported previously (Brewer et al., 1993). They were then plated onto culture dishes coated with 0.1% polyethylenimine at a density of $2.5–5 \times 10^4$ cells/cm^2 for cell survival assay and 10^5 cells/cm^2 for immunoblot analysis.

Fluorescent microscopy

CCL39 cells and primary cultured rat cortical neurons were plated onto collagen-coated glass coverslips and cultivated for 1 d. They were then transiently transfected with the EGFP-Akt/PKB-PH construct together with either NCS-1, E120Q, or pCDNA3 (1:3 ratio) using LipofectAMINE 2000 (Invitrogen) and were subjected to immunocytochemistry. In brief, cells were fixed with 4% PFA, permeabilized with 0.2% Triton X-100, and blocked with 5% BSA. They were then incubated for 1 h with anti–NCS-1 antibody (1:200) followed by incubation with secondary antibodies (FITC- or rhodamine-conjugated goat anti–rabbit IgG; 1:200; Jackson ImmunoResearch Laboratories). After extensive wash with PBS, cell images were scanned on a laser confocal microscope (MRC-1024K; Bio-Rad Laboratories) or obtained with conventional epifluorescence illumination (BX50WI; Olympus) with a cooled CCD camera (CoolSNAP; Photometrics) using a 0.9-W 60× water immersion objective lens. Immunocytochemistry for PC-12 cells were also performed in the same way.

Evaluation of neuronal survival

The primary cultured neurons were infected with viruses at a multiplicity of infection of 100 pfu/cell at 5 d after plating. Under this condition, we found that nearly 70% of the neurons were infected by monitoring EGFP fluorescence (Fig. 3 A). The number of living neurons was counted within the fixed area of images taken by a digital camera (Coolpix 4500; Nikon). To count the number of cells always within the same area, a grid seal with numbering (Asahi Techno glass) was stuck on the bottom of each culture dish. The number of living neurons remaining at each day was expressed as a percentage of the initial number. Neurons showing the degenerating stage characterized by nuclear condensation, membrane blebbing, or extensive neurite fragmentation were excluded. Four different regions were selected from one dish, and six separate experiments were performed for each condition.

To identify and quantify apoptotic neurons, cells were fixed with 4% PFA and were stained with Hoechst 33258. Coverslips were mounted onto glass slides, and cells were observed under epifluorescence illumination on an inverted microscope (1X71; Olympus) using a 40× NA 1.35 oil immersion objective lens (Olympus). Cells were considered apoptotic if their nuclear chromatin was condensed or fragmented, whereas cells were considered viable if their chromatin was diffusely and evenly distributed throughout the nucleus (Fig. 3 F).

Immunoblot analysis

DMV tissue samples were obtained by scratching the DMV neurons from several frozen sections of brainstem (described in the next section) using pulled glass capillary under the light microscope. These tissue samples or cultured cells (PC-12 cells and cortical neurons) were then solubilized in SDS-PAGE sample buffer containing protease and phosphatase inhibitors and subjected to immunoblot analysis using image density software (Scion Image; Scion Corp.) as previously described (Nakamura et al., 2001). Primary antibodies used were anti–NCS-1 antibody (1:1,000), which was previously described (Jeromin et al., 1999), and publicly available antibodies: monoclonal anti-GAPDH antibody (1:1,000) obtained from Chemicon as well as antiphospho-Akt antibodies (detectable for the phosphorylation of Thr308 and Ser473; 1:1,000) and anti-Akt antibody (1:1,000; both from Cell Signaling Technology). Secondary antibodies used were HRP-conjugated anti–rabbit and anti–mouse antibodies or a combination of biotinylated anti–rabbit (or mouse) antibodies (Zymed Laboratories) and HRP-conjugated streptavidin (Zymed Laboratories).

In vivo axotomy and colchicine treatment

The method of vagus axotomy was described previously (Nabekura et al., 2002a). In brief, 4–6-wk-old Sprague-Dawley rats were deeply anesthetized with 50 mg/kg pentobarbital, and axotomy of the vagus motor neurons was performed with fine scissors at the unilateral vagus nerve at the neck. Injured neurons were confirmed by detecting the fluorescence of DiI in the DMV, which had been placed at the proximal cut site of the nerve bundle (Nabekura et al., 2002a).

To test the effects of colchicine, an implantable polymer containing 10% (wt/vol) colchicine was made by mixing colchicine with ethylene-vinyl acetate copolymer (Elvax) followed by drying as described previously (Kakizawa et al., 2000). Solid slices (~1 mm^2) were placed around the unilateral vagal nerve to allow the continuous release of colchicine from slices. The skin incision was closed, and rats were returned to the cage after awaking from the anesthetic.

Histology

1 d to 2 mo (usually 1 wk) after receiving ipsilateral vagal axotomy, brainstems were quickly removed, and 8–10-μm-thick frozen sections were cut. Immunohistochemistry was performed using the labeled biotin–streptavidin method. In brief, after fixation and blocking, the sections were incubated at 4°C overnight with a rabbit polyclonal antibody against NCS-1 at a dilution of 1:15,000 and were sequentially incubated with a biotinylated anti–rabbit secondary antibody and a HRP-conjugated streptavidin–biotin complex (GE Healthcare). The colored reaction product was developed with DAB solution. The sections were lightly counterstained with hematoxylin to visualize nuclei. Images were acquired using a digital camera (FX380; Olympus) equipped with an image filing software (FLVFS-LS; Flovel).

Comparison of the expression level of NCS-1 between injured and control sides were performed using computerized image analysis (Win Roof; Mitani Corp.). In brief, the DMV region from the injured side was at first selected, and the image was converted to binary images by thresholding so that only the area highly stained with anti–NCS-1 antibody could be detected. The same threshold level was used for both the control and injured DMV in each tissue section. The highly stained area was summated and represented as normalized values.

Neuronal degeneration was evaluated by counting surviving neurons as described previously (Rothstein et al., 2005) as well as by TUNEL staining using the apoptag peroxidase in situ Apoptosis Detection Kit (Chemicon). In brief, in vivo axotomy was performed as described above, and, at the same time, adenoviral vectors carrying EGFP only, EGFP plus NCS-1, or E120Q (10^9 pfu each) was injected into the stump of the nerve using a 34-gauge needle. 1 wk after axotomy, paraffin-embedded serial sections (3–4 μm) were made from the brainstem. After they were deparaffinized, sections were directly stained with hematoxylin/eosin to visualize the structure of the DMV region. TUNEL staining was performed in accordance with the manufacturer's method. The sections were lightly counterstained with methyl green. Control sections were treated similarly but incubated in the absence of TdT enzyme. To confirm whether the adenoviral vectors were transferred to the DMV neurons, another set of animals were treated in the same way. 8-μm frozen sections were cut 1 wk after operation, and EGFP signals were viewed under a fluorescence microscope (1X71; Olympus). All image acquisitions were performed at room temperature, and images were subsequently processed using Adobe Photoshop (version 7) and Adobe Illustrator (version 10) software. All experiments conformed to the Guiding Principles for the Care and Use of Animals approved by the Council of the Physiological Society of Japan. All efforts were made to minimize the number of animals used and their suffering.

Statistics

Comparisons between two groups were performed using the paired or unpaired *t* test. Values of $P < 0.05$ were considered statistically significant. All summarized data are expressed as means ± SEM.

We thank Dr. Andrew Moorhouse (The University of New South Wales, Sydney, Australia) for critical reading of this manuscript. We also thank Dr. Takeharu Nishimoto and Dr. Hideo Nishitani (Kyushu University, Fukuoka, Japan) for useful discussions of this study.

This work was supported, in part, by a Grant-in-Aid for Scientific Research (17590196) and Priority Areas (13142210) from the Ministry of Education, Culture, Sports, Science and Technology of Japan and the Japan Heart Foundation and by a grant from the National Institutes of Health/National Institute of Neurological Disorder and Stroke (NS38126).

Submitted: 24 August 2005
Accepted: 17 February 2006

References

Alessi, D.R., M. Andjelkovic, B. Caudwell, P. Cron, N. Morrice, P. Cohen, and B.A. Hemmings. 1996. Mechanism of activation of protein kinase B by insulin and IGF-1. *EMBO J.* 15:6541–6551.

Benn, S.C., and C.J. Woolf. 2004. Adult neuron survival strategies–slamming on the brakes. *Nat. Rev. Neurosci.* 5:686–700.

Boyd, J.G., and T. Gordon. 2003. Neurotrophic factors and their receptors in axonal regeneration and functional recovery after peripheral nerve injury. *Mol. Neurobiol.* 27:277–324.

Brewer, G.J. 1995. Serum-free B27/neurobasal medium supports differentiated growth of neurons from the striatum, substantia nigra, septum, cerebral cortex, cerebellum, and dentate gyrus. *J. Neurosci. Res.* 42:674–683.

Brewer, G.J., J.R. Torricelli, E.K. Evege, and P.J. Price. 1993. Optimized survival of hippocampal neurons in B27-supplemented Neurobasal, a new serum-free medium combination. *J. Neurosci. Res.* 35:567–576.

Cantley, L.C. 2002. The phosphoinositide 3-kinase pathway. *Science.* 296:1655–1657.

Chen, X.L., Z.G. Zhong, S. Yokoyama, C. Bark, B. Meister, P.O. Berggren, J. Roder, H. Higashida, and A. Jeromin. 2001. Overexpression of rat neuronal calcium sensor-1 in rodent NG108-15 cells enhances synapse formation and transmission. *J. Physiol.* 532:649–659.

Cheng, A., S. Wang, D. Yang, R. Xiao, and M.P. Mattson. 2003. Calmodulin mediates brain-derived neurotrophic factor cell survival signaling upstream of Akt kinase in embryonic neocortical neurons. *J. Biol. Chem.* 278:7591–7599.

Currie, R.A., K.S. Walker, A. Gray, M. Deak, A. Casamayor, C.P. Downes, P. Cohen, D.R. Alessi, and J. Lucocq. 1999. Role of phosphatidylinositol 3,4,5-trisphosphate in regulating the activity and localization of 3-phosphoinositide-dependent protein kinase-1. *Biochem. J.* 337:575–583.

Gomez, M., E. De Castro, E. Guarin, H. Sasakura, A. Kuhara, I. Mori, T. Bartfai, C.I. Bargmann, and P. Nef. 2001. Ca^{2+} signaling via the neuronal calcium sensor-1 regulates associative learning and memory in *C. elegans*. *Neuron.* 30:241–248.

Henderson, C.E., H.S. Phillips, R.A. Pollock, A.M. Davies, C. Lemeulle, M. Armanini, L. Simmons, B. Moffet, R.A. Vandlen, L.C. Simpson, et al. 1994. GDNF: a potent survival factor for motoneurons present in peripheral nerve and muscle. *Science.* 266:1062–1064.

Hendricks, K.B., B.Q. Wang, E.A. Schnieders, and J. Thorner. 1999. Yeast homologue of neuronal frequenin is a regulator of phosphatidylinositol-4-OH kinase. *Nat. Cell Biol.* 1:234–241.

Jeromin, A., A.J. Shayan, M. Msghina, J. Roder, and H.L. Atwood. 1999. Crustacean frequenins: molecular cloning and differential localization at neuromuscular junctions. *J. Neurobiol.* 41:165–175.

Jeromin, A., D. Muralidhar, M.N. Parameswaran, J. Roder, T. Fairwell, S. Scarlata, L. Dowal, S.M. Mustafi, K.V. Chary, and Y. Sharma. 2004. N-terminal myristoylation regulates calcium-induced conformational changes in neuronal calcium sensor-1. *J. Biol. Chem.* 279:27158–27167.

Kakizawa, S., M. Yamasaki, M. Watanabe, and M. Kano. 2000. Critical period for activity-dependent synapse elimination in developing cerebellum. *J. Neurosci.* 20:4954–4961.

Kirik, D., B. Georgievska, and A. Bjorklund. 2004. Localized striatal delivery of GDNF as a treatment for Parkinson disease. *Nat. Neurosci.* 7:105–110.

Kiryu-Seo, S., M. Sasaki, H. Yokohama, S. Nakagomi, T. Hirayama, S. Aoki, K. Wada, and H. Kiyama. 2000. Damage-induced neuronal endopeptidase (DINE) is a unique metallopeptidase expressed in response to neuronal damage and activates superoxide scavengers. *Proc. Natl. Acad. Sci. USA.* 97:4345–4350.

Koh, P.O., A.S. Undie, N. Kabbani, R. Levenson, P.S. Goldman-Rakic, and M.S. Lidow. 2003. Up-regulation of neuronal calcium sensor-1 (NCS-1) in the prefrontal cortex of schizophrenic and bipolar patients. *Proc. Natl. Acad. Sci. USA.* 100:313–317.

Koizumi, S., P. Rosa, G.B. Willars, R.A. Challiss, E. Taverna, M. Francolini, M.D. Bootman, P. Lipp, K. Inoue, J. Roder, and A. Jeromin. 2002. Mechanisms underlying the neuronal calcium sensor-1-evoked enhancement of exocytosis in PC12 cells. *J. Biol. Chem.* 277:30315–30324.

Korhonen, L., I. Hansson, J.P. Kukkonen, K. Brannvall, M. Kobayashi, K. Takamatsu, and D. Lindholm. 2005. Hippocalcin protects against caspase-12-induced and age-dependent neuronal degeneration. *Mol. Cell. Neurosci.* 28:85–95.

Liberatore, G.T., J.Y. Wong, M.J. Porritt, G.A. Donnan, and D.W. Howells. 1997. Expression of glial cell line-derived neurotrophic factor (GDNF) mRNA following mechanical injury to mouse striatum. *Neuroreport.* 8:3097–3101.

Liston, P., W.G. Fong, and R.G. Korneluk. 2003. The inhibitors of apoptosis: there is more to life than Bcl2. *Oncogene.* 22:8568–8580.

Mallart, A., D. Angaut-Petit, C. Bourret-Poulain, and A. Ferrus. 1991. Nerve terminal excitability and neuromuscular transmission in T(X;Y)V7 and Shaker mutants of *Drosophila melanogaster*. *J. Neurogenet.* 7:75–84.

Mercer, E.A., L. Korhonen, Y. Skoglosa, P.A. Olsson, J.P. Kukkonen, and D. Lindholm. 2000. NAIP interacts with hippocalcin and protects neurons against calcium-induced cell death through caspase-3-dependent and -independent pathways. *EMBO J.* 19:3597–3607.

Nabekura, J., T. Ueno, S. Katsurabayashi, A. Furuta, N. Akaike, and M. Okada. 2002a. Reduced NR2A expression and prolonged decay of NMDA receptor-mediated synaptic current in rat vagal motoneurons following axotomy. *J. Physiol.* 539:735–741.

Nabekura, J., T. Ueno, A. Okabe, A. Furuta, T. Iwaki, C. Shimizu-Okabe, A. Fukuda, and N. Akaike. 2002b. Reduction of KCC2 expression and GABAA receptor-mediated excitation after in vivo axonal injury. *J. Neurosci.* 22:4412–4417.

Nakamura, T.Y., D.J. Pountney, A. Ozaita, S. Nandi, S. Ueda, B. Rudy, and W.A. Coetzee. 2001. A role for frequenin, a Ca^{2+}-binding protein, as a regulator of Kv4 K^+-currents. *Proc. Natl. Acad. Sci. USA.* 98:12808–12813.

Nakamura, T.Y., E. Sturm, D.J. Pountney, B. Orenzoff, M. Artman, and W.A. Coetzee. 2003. Developmental expression of NCS-1 (frequenin), a regulator of Kv4 K^+ channels, in mouse heart. *Pediatr. Res.* 53:554–557.

Nicole, O., C. Ali, F. Docagne, L. Plawinski, E.T. MacKenzie, D. Vivien, and A. Buisson. 2001. Neuroprotection mediated by glial cell line-derived neurotrophic factor: involvement of a reduction of NMDA-induced calcium influx by the mitogen-activated protein kinase pathway. *J. Neurosci.* 21:3024–3033.

Olafsson, P., T. Wang, and B. Lu. 1995. Molecular cloning and functional characterization of the *Xenopus* Ca^{2+}-binding protein frequenin. *Proc. Natl. Acad. Sci. USA.* 92:8001–8005.

Oppenheim, R.W., L.J. Houenou, J.E. Johnson, L.F. Lin, L. Li, A.C. Lo, A.L. Newsome, D.M. Prevette, and S. Wang. 1995. Developing motor neurons rescued from programmed and axotomy-induced cell death by GDNF. *Nature.* 373:344–346.

Perez-Garcia, M.J., V. Cena, Y. de Pablo, M. Llovera, J.X. Comella, and R.M. Soler. 2004. Glial cell line-derived neurotrophic factor increases intracellular calcium concentration. Role of calcium/calmodulin in the activation of the phosphatidylinositol 3-kinase pathway. *J. Biol. Chem.* 279:6132–6142.

Perrelet, D., A. Ferri, P. Liston, P. Muzzin, R.G. Korneluk, and A.C. Kato. 2002. IAPs are essential for GDNF-mediated neuroprotective effects in injured motor neurons in vivo. *Nat. Cell Biol.* 4:175–179.

Pongs, O., J. Lindemeier, X.R. Zhu, T. Theil, D. Engelkamp, I. Krah-Jentgens, H.G. Lambrecht, K.W. Koch, J. Schwemer, R. Rivosecchi, et al. 1993. Frequenin–a novel calcium-binding protein that modulates synaptic efficacy in the *Drosophila* nervous system. *Neuron.* 11:15–28.

Rothstein, J.D., S. Patel, M.R. Regan, C. Haenggeli, Y.H. Huang, D.E. Bergles, L. Jin, M. Dykes Hoberg, S. Vidensky, D.S. Chung, et al. 2005. Beta-lactam antibiotics offer neuroprotection by increasing glutamate transporter expression. *Nature.* 433:73–77.

Sippy, T., A. Cruz-Martin, A. Jeromin, and F.E. Schweizer. 2003. Acute changes in short-term plasticity at synapses with elevated levels of neuronal calcium sensor-1. *Nat. Neurosci.* 6:1031–1038.

Soler, R.M., X. Dolcet, M. Encinas, J. Egea, J.R. Bayascas, and J.X. Comella. 1999. Receptors of the glial cell line-derived neurotrophic factor family of neurotrophic factors signal cell survival through the phosphatidylinositol 3-kinase pathway in spinal cord motoneurons. *J. Neurosci.* 19:9160–9169.

Takahashi, M. 2001. The GDNF/RET signaling pathway and human diseases. *Cytokine Growth Factor Rev.* 12:361–373.

Tsujimoto, T., A. Jeromin, N. Saitoh, J.C. Roder, and T. Takahashi. 2002. Neuronal calcium sensor 1 and activity-dependent facilitation of P/Q-type calcium currents at presynaptic nerve terminals. *Science.* 295:2276–2279.

Wang, C.Y., F. Yang, X. He, A. Chow, J. Du, J.T. Russell, and B. Lu. 2001. Ca^{2+} binding protein frequenin mediates GDNF-induced potentiation of Ca^{2+} channels and transmitter release. *Neuron.* 32:99–112.

Wang, Y., C.F. Chang, M. Morales, Y.H. Chiang, and J. Hoffer. 2002. Protective effects of glial cell line-derived neurotrophic factor in ischemic brain injury. *Ann. NY Acad. Sci.* 962:423–437.

Weiss, J.L., D.A. Archer, and R.D. Burgoyne. 2000. Neuronal Ca^{2+} sensor-1/frequenin functions in an autocrine pathway regulating Ca^{2+} channels in bovine adrenal chromaffin cells. *J. Biol. Chem.* 275:40082–40087.

Weisz, O.A., G.A. Gibson, S.M. Leung, J. Roder, and A. Jeromin. 2000. Overexpression of frequenin, a modulator of phosphatidylinositol 4-kinase, inhibits biosynthetic delivery of an apical protein in polarized madin-darby canine kidney cells. *J. Biol. Chem.* 275:24341–24347.

Yamamoto, M., N. Mitsuma, Y. Ito, N. Hattori, M. Nagamatsu, M. Li, T. Mitsuma, and G. Sobue. 1998. Expression of glial cell line-derived neurotrophic factor and GDNFR-alpha mRNAs in human peripheral neuropathies. *Brain Res.* 809:175–181.

Yan, Q., C. Matheson, and O.T. Lopez. 1995. In vivo neurotrophic effects of GDNF on neonatal and adult facial motor neurons. *Nature.* 373:341–344.